

## Field-induced gapless electron pocket in the superconducting vortex phase of $\text{YNi}_2\text{B}_2\text{C}$ as probed by magnetoacoustic quantum oscillations

J. Nössler,<sup>1,2</sup> R. Seerig,<sup>1,2</sup> S. Yasin,<sup>1</sup> M. Uhlarz,<sup>1</sup> S. Zherlitsyn,<sup>1</sup> G. Behr,<sup>3,\*</sup> S.-L. Drechsler,<sup>3</sup>  
G. Fuchs,<sup>3</sup> H. Rosner,<sup>4</sup> and J. Wosnitzer<sup>1,2</sup>

<sup>1</sup>*Hochfeld-Magnetlabor Dresden (HLD-EMFL), Helmholtz-Zentrum Dresden-Rossendorf, 01314 Dresden, Germany*

<sup>2</sup>*Institut für Festkörperphysik, TU Dresden, 01062 Dresden, Germany*

<sup>3</sup>*Leibniz Institute for Solid State and Materials Research, IFW Dresden, 01171 Dresden, Germany*

<sup>4</sup>*Max Planck Institute for Chemical Physics of Solids, 01187 Dresden, Germany*

(Received 7 November 2016; revised manuscript received 15 January 2017; published 30 January 2017)

By use of ultrasound studies we resolved magnetoacoustic quantum oscillation deep into the mixed state of the multiband nonmagnetic superconductor  $\text{YNi}_2\text{B}_2\text{C}$ . Below the upper critical field, only a very weak additional damping appears that can be well explained by the field inhomogeneity caused by the flux-line lattice in the mixed state. This is clear evidence for no or a vanishingly small gap for one of the bands, namely, the spheroidal  $\alpha$  band. This contrasts de Haas–van Alphen data obtained by use of torque magnetometry for the same sample, with a rapidly vanishing oscillation signal in the mixed state. This points to a strongly distorted flux-line lattice in the latter case that, in general, can hamper a reliable extraction of gap parameters by use of such techniques.

DOI: [10.1103/PhysRevB.95.014523](https://doi.org/10.1103/PhysRevB.95.014523)

The observation of magnetic quantum oscillations is usually taken as evidence for the existence of a Fermi surface. The appearance of Landau levels in a magnetic field leads to an oscillating density of states at the Fermi level as a function of field. Experimentally, these oscillations can be detected in many thermodynamic and transport properties, with the most prominent being the de Haas–van Alphen (dHvA) effect in the magnetization. Consequently, the observation of dHvA oscillations in the mixed state of a superconductor first appeared as a surprise [1]. Below the upper critical field,  $B_{c2}$ , the opening of a superconducting gap and the corresponding disappearance of the entire Fermi surface seem to contradict the existence of such oscillations. Nevertheless, they were observed in many type-II superconductors ([2–4] and references therein).

Motivated by the experimental evidence, however, it subsequently was shown by a number of theoretical studies that this phenomenon may be understood in principle in a rather general context. Thereby, different models are used to explain the occurrence of quantum oscillations below  $B_{c2}$  [5–9], but it still remains unclear which of them is the most appropriate. Usually, the validity of these theories is tested by comparing the predicted additional damping of the quantum oscillations below  $B_{c2}$  with experiment. Such analysis gives as the main fit parameter the superconducting gap at zero temperature,  $\Delta_0$ , a value that largely depends on the used model.

With the proper theory at hand dHvA data could, in principle, yield information on the field and angular evolution of the superconducting gap,  $\Delta$ . However, considerable ambiguity in  $\Delta$  is introduced not only by the various theoretical predictions but even more from varying, sometimes contradictory, experimental data. In particular, for  $\text{YNi}_2\text{B}_2\text{C}$  and  $\text{LuNi}_2\text{B}_2\text{C}$  highly controversial results were reported [4,10–18]. Thereby, for the so-called  $\alpha$  band, an additional damping of the dHvA signal was found either in line with the opening of a weak-coupling gap [11–13,15], or yielding an unexpectedly

small gap [4,10,14,17,18], or even an abrupt vanishing of the oscillations below  $B_{c2}$  [16]. All these experimental results were obtained by measuring the dHvA effect by use of either the torque or the field-modulation method.

Here, we present quantum-oscillation data obtained for  $\text{YNi}_2\text{B}_2\text{C}$  by use of ultrasound measurements comparing them to magnetic-torque data. By studying the magnetoacoustic quantum oscillations in the normal and superconducting state we find a marginal additional damping of the oscillations below  $B_{c2}$ , that can be ascribed solely to the expected magnetic-field inhomogeneities originating from a regular flux-line lattice, evidencing a vanishingly small or even the absence of a gap on the  $\alpha$  band. This contrasts the abrupt vanishing of the torque dHvA signal measured for the same sample.

Recently, Gor'kov [19] argued that small gaps can be induced from dominant large, strongly interacting Fermi surfaces onto small, minor bands of multiband superconductors. He explicitly mentioned  $\text{YNi}_2\text{B}_2\text{C}$  as one candidate among others. Furthermore, Barzykin [20] and Barzykin and Gor'kov [21], based on a simplified analysis of two special BCS-type two-band models, proposed the possibility of a partial quenching of superconductivity by an external magnetic field, i.e., a gapless state in weakly coupled bands at low temperatures for multiband superconductors. Here, we provide further general arguments for such a scenario, focusing on the case of a small weakly coupled pocket relevant for  $\text{YNi}_2\text{B}_2\text{C}$ .

Superconductivity in  $R\text{Ni}_2\text{B}_2\text{C}$  ( $R$  = rare earth) was discovered more than 20 years ago [22,23] and immediately received considerable attention. (For recent reviews see [24,25].) The unusual properties in the superconducting state led to controversial debates on its nature. In particular, these materials were among the first for which multiband superconductivity was detected [26–29]. Furthermore, pronounced gap anisotropies have been suggested [30,31]. In previous dHvA studies in the normal state, band- and angular-dependent mass enhancements evidenced largely varying coupling strengths for and within the various bands of  $\text{LuNi}_2\text{B}_2\text{C}$  [18,29]. Angular-resolved photoemission-spectroscopy data as well revealed highly anisotropic and band-dependent gaps in  $\text{YNi}_2\text{B}_2\text{C}$  [32].

\*Deceased.

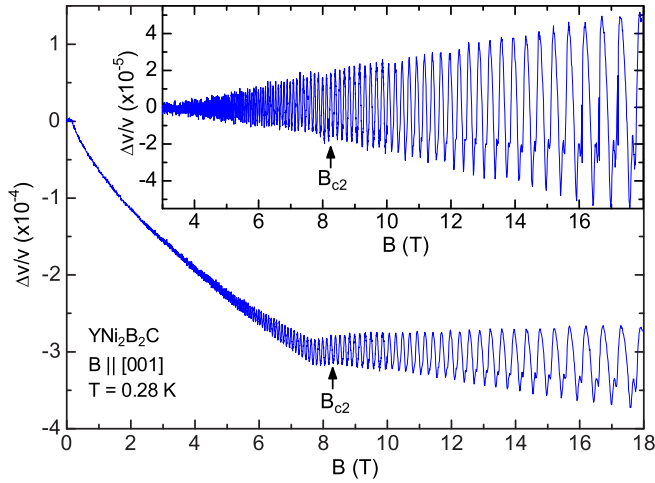


FIG. 1. Magnetic-field dependence of the relative change of the longitudinal sound velocity for sound propagating along the  $c$  axis in  $\text{YNi}_2\text{B}_2\text{C}$  measured at 0.28 K in fields up to 18 T aligned as well along  $c$ . The inset shows the oscillating part of the signal after background subtraction.

High-quality  $\text{YNi}_2\text{B}_2\text{C}$  single crystals were grown by a zone-melting method [33,34], improved by optical heating. From the resulting rod a piece (HKZ066-A) with dimensions  $2.64 \times 1.63 \times 1.365 \text{ mm}^3$  has been cut out that successively was annealed at  $900^\circ\text{C}$ . This sample was then investigated using ultrasound and magnetic-torque measurements. It has a superconducting transition temperature  $T_c = 15.3(1) \text{ K}$  with a transition width of about 0.1 K and a resistance ratio between 300 and 16 K of 39.

The ultrasound data were taken using a phase-sensitive detection technique that allowed us to measure the relative changes of the sound velocity,  $\Delta v/v$ , and the sound attenuation (not discussed further here) [35]. Thin-film transducers for longitudinally polarized sound waves propagating at a frequency of 71.3 MHz along the  $c$  direction were glued to the polished ends of the sample. The measurements were done using a  $^3\text{He}$  cryostat placed inside an 18/20 T superconducting magnet. The dHvA signal was measured by use of a capacitive cantilever immersed in the  $^3\text{He}$  of a toploading cryostat in magnetic fields up to 13 T. For that, the same sample was glued by a small amount of Apiezon-N grease onto a  $50\text{-}\mu\text{m}$ -thick copper-beryllium cantilever.

The relative change of the sound velocity in  $\text{YNi}_2\text{B}_2\text{C}$  measured at 280 mK is shown in Fig. 1. On a smoothly varying background signal clear quantum oscillations are visible. With increasing magnetic field in the superconducting state, the background sound velocity decreases (lattice softening) until at  $B_{c2} \approx 8.25 \text{ T}$  a small anomaly appears [36], above which the background stays nearly constant. After subtracting this background the magnetic quantum oscillations, resolvable above about 3 T, are nicely seen in the inset of Fig. 1. The frequency of this oscillation,  $F_\alpha = 505(1) \text{ T}$ , agrees well with previous dHvA results [10,11,13–15,37,38] and has been ascribed to a small spheroidal Fermi-surface pocket centered around the  $\Gamma$  point of the Brillouin zone [39]. The amplitude of the oscillating signals smoothly grows with increasing field without any obvious anomalous changes when going from the mixed to

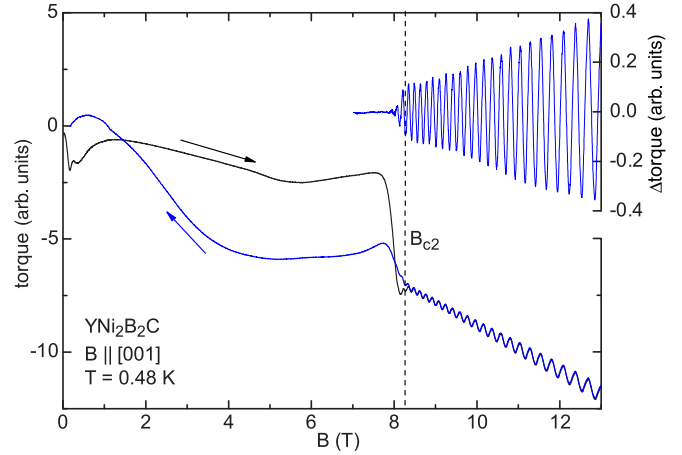


FIG. 2. Field dependence of the magnetic torque of  $\text{YNi}_2\text{B}_2\text{C}$ . Up and down sweeps are shown (indicated by arrows) for fields aligned nearly parallel to  $c$ . In the upper right of the panel the background-subtracted signal is shown.

the normal-conducting state. No hysteresis could be observed between up and down field sweeps in the ultrasound data.

This is largely different for the dHvA signal of the same sample in the torque data (Fig. 2). In the normal state, the frequency  $F_\alpha$  is well resolvable with smoothly decreasing amplitude down to  $B_{c2}$ . In the mixed state, however, the oscillations abruptly vanish (inset of Fig. 2). In the as-measured torque signal a large hysteresis and peak effect occurs. Such behavior is well known from previous studies [14,16,40]. Nevertheless, the present data allow for a reliable subtraction of the background signal evidencing the extremely rapid disappearance of the dHvA signal below  $B_{c2}$ .

Such a fast vanishing of the dHvA in the mixed state, reported previously as well in Ref. [16], is very unexpected and cannot be reasonably explained by the opening of a superconducting gap. The latter is clearly proven by our ultrasound data for which quantum oscillations persist deep into the mixed state. On the reason for this strong damping of the torque dHvA signal we can only speculate at the moment. A possible scenario is the existence of a strongly disordered vortex arrangement in the torque experiments. This disorder then leads to pronounced field inhomogeneities within the sample. Further evidence for strong disorder in the vortex lattice is given by the large peak effect appearing in the magnetization, especially close to  $B_{c2}$ . This peak effect is connected with a massive rearrangement of vortices within the sample. Such a feature is expected to be strongly sample dependent as indeed seen experimentally [4,10–18]. For the ultrasound measurements the persistence of the magnetic quantum oscillations down to very low fields in the mixed state proves that in this case no strong field inhomogeneities exist. This might be caused by the sound waves distorting the crystallographic lattice and leading thereby to a rearrangement of the vortices into a regular lattice. In this context, one may refer to earlier vortex-shaking experiments, where the application of an additional oscillating magnetic field leads to a fast depinning of the vortex lattice [41–44]. Although sound waves do not directly shake vortices, they shake pinning centers which in return could rearrange the vortices.

Anyway, the direct comparison between torque and ultrasound data on the same sample evidences that the strong damping in the torque dHvA signal below  $B_{c2}$  cannot be related to an intrinsic opening of a superconducting gap. Indeed, when analyzing the additional damping of the dHvA signal using Eq. (3), discussed in detail below, an unphysical huge zero-temperature gap of  $\Delta_0 \approx 25$  meV would result. This contrasts the oscillating ultrasound signal that favorably can be analyzed invoking reasonable damping factors.

The field-dependent damping of magnetic quantum oscillations is usually described by factors [2,45,46]

$$R_i = \exp\left(-\frac{\pi m_c}{eB\tau_i}\right), \quad (1)$$

with  $e$  the electron charge,  $m_c$  the cyclotron effective mass extracted from the temperature-dependent damping of the quantum oscillations [47], and  $\tau_i$  the various ‘‘scattering times’’ explained below. We obtain  $m_c = 0.34(1)m_e$  for the  $\alpha$  orbit, with  $m_e$  the free-electron mass, both from our torque and ultrasound data. This nicely agrees with previous reports [10,13,14]. In the mixed state, the effective mass does not change within error bars as obtained from our ultrasound data.

In the normal-conducting state, the relevant factor is the Dingle damping,  $R_D$ , with the electronic scattering time  $\tau_D = \hbar/(2\pi k_B T_D)$ , where  $k_B$  is the Boltzmann constant. The Dingle temperature  $T_D$  provides a measure of the scattering rate within a certain sample and band. When plotting the amplitudes,  $A$ , of the magnetic quantum oscillations with appropriate scalings in a Dingle plot [48],  $T_D$  is easily extracted from a linear fit to the data above  $B_{c2}$  (dashed lines in Fig. 3). We find  $T_D = 1.9(1)$  K for the ultrasound and  $T_D = 2.6(4)$  K for the torque data. The larger error bar for the latter data originates in the limited available fit range.

In Fig. 3, again the striking difference of the damping in the mixed state is apparent: In the torque measurement, the amplitude vanishes abruptly within two or three oscillation periods [Fig. 3(b)]. Note that here the field-dependent amplitudes were determined by Fourier transformation over three oscillation periods and shifting this window consecutively by one period. In the ultrasound data [Fig. 3(a)], only a very small additional damping appears below  $B_{c2}$ . One reason for such a damping is the always present field inhomogeneity caused by the vortex lattice. This can be described by the damping factor  $R_{FL}$  [2], containing the scattering rate

$$\tau_{FL}^{-1} = \sqrt{\frac{\pi F}{2}} \frac{e}{\pi \kappa^2 m_c} \frac{B_{c2} - B}{\sqrt{B}}, \quad (2)$$

where  $\kappa$  is the Ginzburg-Landau parameter and  $F$  is the dHvA frequency ( $F_\alpha$  here). Strictly speaking, this derivation is valid only close to  $B_{c2}$  and for an ideal hexagonal flux-line lattice [49]. For  $\text{YNi}_2\text{B}_2\text{C}$ ,  $\kappa$  values between 10 and 15 are reported [50,51]. Using  $\kappa = 12$ , we can already well account for the additional damping seen in the magnetoacoustic quantum oscillations [solid line in Fig. 3(a)]. Here, we have, however, not yet considered any damping due to the opening of a superconducting gap.

In fact, in case such a gap would open over the detected  $\alpha$  pocket further damping of the oscillating signal would be

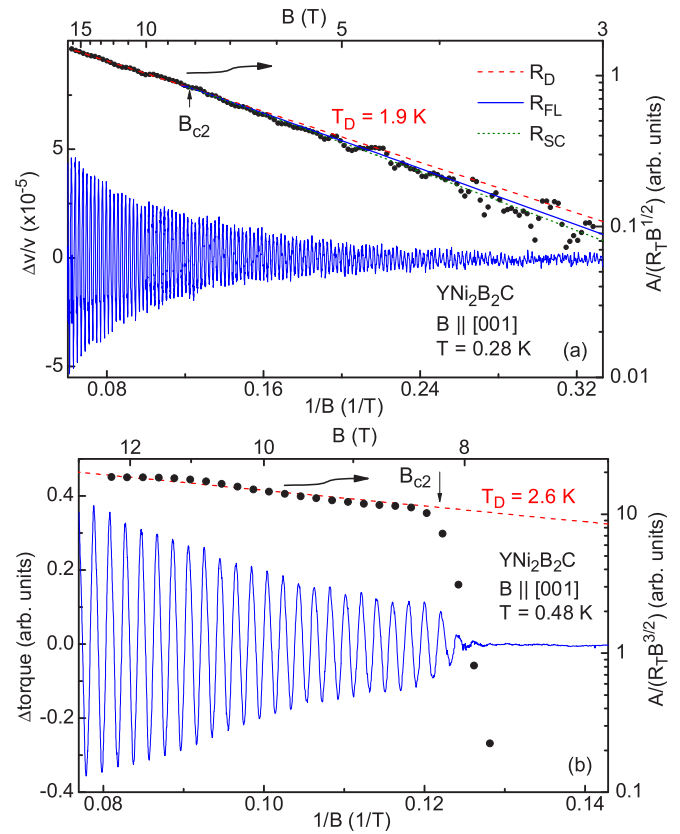


FIG. 3. (a) Magnetoacoustic quantum oscillations (see also the inset of Fig. 1) together with a Dingle plot of the oscillation amplitude (right axis) as a function of  $1/B$ . The dashed line is a fit to the Dingle data in the normal state. For the solid and dotted lines see main text. (b) The same kind of plot for the dHvA data measured by use of the torque method (Fig. 2) with fit (dashed line) to the normal-state Dingle data.

expected. All theories considering this gap opening predict a considerable additional damping [2,3,5–9]. Thereby, most of these theories are valid only close to  $B_{c2}$ . An often used approach to describe the additional damping in the superconducting state is that introduced by Maki which results in the damping term  $R_{SC}$  as given by Eq. (1) with scattering rate [5]

$$\tau_{SC}^{-1} = \Delta^2 \frac{m_c}{e\hbar B} \sqrt{\frac{\pi B}{F}}, \quad (3)$$

where  $\Delta$  is the field-dependent superconducting gap averaged over the cyclotron orbit. With the usual approximation  $\Delta = \Delta_0 \sqrt{1 - B/B_{c2}}$ , the only fit parameter is  $\Delta_0$ . For the total damping, now consisting of  $R_D$ ,  $R_{FL}$ , and  $R_{SC}$ , we obtain a maximum gap of  $\Delta_0 \approx 0.6$  meV [52]. This total damping is shown by the dotted line in Fig. 3(a). In the weak-coupling limit,  $\Delta_0 = 1.764 k_B T_c \approx 2.33$  meV would be expected, in accord with the  $\alpha$ -band-gap value obtained in a recent *ab initio* study [31]. We emphasize here that the factor  $R_{SC}$  is not necessary to describe the ultrasound data; even with  $R_{SC} = 1$  ( $\Delta_0 = 0$ ) the fit is excellent.

A possible scenario explaining our experimental observation, using a realistic multiband approach sketched below,

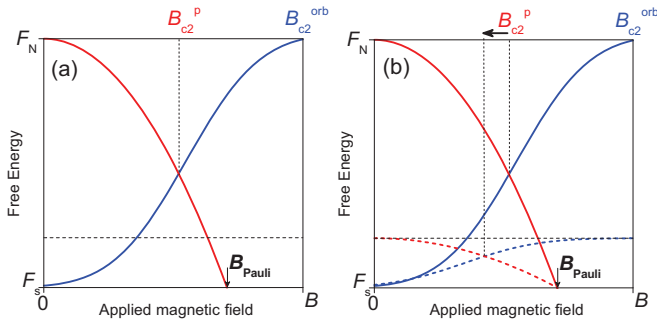


FIG. 4. (a) Schematic view of the determination of  $B_{c2}$  from the energy-gain balance between the condensation and field penetration for a single-band superconductor, after [53,54]. (b) The same for an artificially isolated weakly coupled band of a multiband superconductor with almost vanishing interband coupling to the dominant band which is still approximately described as in (a) [55].

is the field-induced quenching of superconductivity in the  $\alpha$  pocket well below  $B_{c2}$ . As mentioned in the introduction such behavior may occur in multiband superconductors for a weakly with otherwise strongly coupled bands [20,21]. A schematic sketch elucidating the quenching of superconductivity, i.e., the reduction of the critical field in a weakly coupled band, is shown in Fig. 4. In order to estimate such a reduced critical field,  $B_{c2}^\alpha(0)$ , we employ a generalized band-specific expression derived within isotropic Eliashberg theory [56], valid here for  $B \parallel c$ :

$$B_{c2,c}^\alpha(0) \approx K \frac{T_c^2(1 + \lambda_\alpha)^{2.4}}{v_{F,\alpha,ab}^2} \left( 1 + \frac{0.13\gamma_{imp}}{T_c(1 + \lambda_\alpha)} \right), \quad (4)$$

where  $\lambda_\alpha$  is the effective  $\alpha$ -band coupling constant,  $v_{F,\alpha,ab}$  is the  $\alpha$ -band Fermi velocity in the  $ab$  plane,  $\gamma_{imp} \approx 2\pi T_D \approx 12$  K is the impurity scattering rate, and the prefactor  $K = k_B^2 \pi^2 \exp(2 - \gamma)/(2\hbar e) = 2.31 \times 10^8$  V/(K<sup>2</sup>s), with the Euler constant  $\gamma = 0.577$ . Using the experimental  $T_c = 15.3$  K, the renormalized Fermi velocity  $v_{F,\alpha,ab}/(1 + \lambda_\alpha) \approx 4.19 \times 10^5$  m/s from dHvA measurements [57], and a reasonable range of  $\lambda_\alpha$

between 0.51 and 1.35 [58], in accord with [31], rather modest  $B_{c2,c}^\alpha(0)$  values between 0.39 and 0.45 T are obtained. This estimate implies that superconductivity in the  $\alpha$  pocket should be quenched for fields well below 3 T above which the dHvA oscillations can be resolved.

A more quantitative self-consistent multiband description within this scenario is outside the scope of the present work and will be considered elsewhere. Anyhow, our suggested weak interband-coupling clean-limit scenario provides additional support for the quenching of a small Fermi-surface pocket in already weak fields. Hence, in the mixed state the  $\alpha$  pocket of YNi<sub>2</sub>B<sub>2</sub>C has indeed very likely a vanishingly small or zero gap while (most of) the other Fermi-surface sheets develop gaps in the superconducting state. These gaps have varying, anisotropic, and partially large values for the different bands as was evidenced by various studies [26–28,59]. Further, we suggest that a similar field-induced quenching mechanism might resolve the puzzle of the accidental point nodes ( $s+g$  wave) proposed by Maki *et al.* [60] based on thermal conductivity [61] and NMR [62] studies performed in fields above 1 T.

In conclusion, we found strong experimental evidence, well supported by theoretical arguments, for the existence of a gapless or, at least, marginally small gapped band in the mixed state of YNi<sub>2</sub>B<sub>2</sub>C. This is proven by our magnetoacoustic quantum-oscillation data that persist deep into the mixed state. It also contrasts our torque dHvA data that would suggest an unphysical large gap. The latter most likely is caused by a strongly disordered flux-line arrangement in the sample. Our results emphasize that, in general, great care is needed when superconducting gap values are being extracted from magnetic quantum oscillations, especially when the flux-line distribution is strongly distorted. Finally, our quenching approach is of interest as well for other multiband superconductors, such as the iron-based materials, having dominant and minor bands, too.

Support by HLD at HZDR, member of the European Magnetic Field Laboratory; by the Deutsche Forschungsgemeinschaft priority program SPP 1485; by the German-Russian-Ukrainian research project by the Volkswagen-Stiftung; and discussions with S. Johnston, D. Efremov, V. Grinenko, and Y. Naidyuk are acknowledged.

- 
- [1] J. E. Graebner and M. Robbins, *Phys. Rev. Lett.* **36**, 422 (1976).  
[2] T. J. B. M. Janssen, C. Haworth, S. M. Hayden, P. Meeson, M. Springford, and A. Wasserman, *Phys. Rev. B* **57**, 11698 (1998).  
[3] T. Maniv, V. Zhuravlev, I. Vagner, and P. Wyder, *Rev. Mod. Phys.* **73**, 867 (2001).  
[4] B. Bergk, S.-L. Drechsler, P. C. Canfield, and J. Wosnitza, *Eur. Phys. J. B* **85**, 57 (2012).  
[5] K. Maki, *Phys. Rev. B* **44**, 2861 (1991).  
[6] P. Miller and B. L. Györfy, *J. Phys.: Condens. Matter* **7**, 5579 (1995).  
[7] K. Miyake, *Physica B* **186-188**, 115 (1993).  
[8] S. Dukan and Z. Tesanovic, *Phys. Rev. Lett.* **74**, 2311 (1995).  
[9] K. Yasui and T. Kita, *Phys. Rev. B* **66**, 184516 (2002).  
[10] M. Heinecke and K. Winzer, *Z. Phys. B* **98**, 147 (1995).  
[11] G. Goll, M. Heinecke, A. G. M. Jansen, W. Joss, L. Nguyen, E. Steep, K. Winzer, and P. Wyder, *Phys. Rev. B* **53**, R8871 (1996).  
[12] G. Goll, L. Nguyen, E. Steep, A. G. M. Jansen, P. Wyder, and K. Winzer, *Physica B* **230-232**, 868 (1997).  
[13] T. Terashima, H. Takeya, S. Uji, K. Kadowaki, and H. Aoki, *Solid State Commun.* **96**, 459 (1995).  
[14] T. Terashima, C. Haworth, H. Takeya, S. Uji, H. Aoki, and K. Kadowaki, *Phys. Rev. B* **56**, 5120 (1997).  
[15] D. Bintley and P. J. Meeson, *Physica C* **388-389**, 181 (2003).  
[16] O. Ignatchik, T. Coffey, J. Hagel, M. Jäckel, E. Jobiliong, D. Souptel, G. Behr, and J. Wosnitza, *J. Magn. Magn. Mater.* **290-291**, 424 (2005).

- [17] B. Bergk, O. Ignatchik, A. D. Bianchi, M. Jäckel, J. Wosnitza, J. Perenboom, and P. C. Canfield, *Physica C* **460-462**, 630 (2007).
- [18] T. Isshiki, N. Kimura, H. Aoki, T. Terashima, S. Uji, K. Yamauchi, H. Harima, D. Jaiswal-Nagar, S. Ramakrishnan, and A. K. Grover, *Phys. Rev. B* **78**, 134528 (2008).
- [19] L. P. Gor'kov, *Phys. Rev. B* **86**, 060501(R) (2012).
- [20] V. Barzykin, *Phys. Rev. B* **79**, 134517 (2009).
- [21] V. Barzykin and L. P. Gor'kov, *Phys. Rev. Lett.* **98**, 087004 (2007); *Phys. Rev. B* **76**, 014509 (2007).
- [22] R. Nagarajan, C. Mazumdar, Z. Hossain, S. K. Dhar, K. V. Gopalakrishnan, L. C. Gupta, C. Godart, B. D. Padalia, and R. Vijayaraghavan, *Phys. Rev. Lett.* **72**, 274 (1994).
- [23] R. J. Cava, H. Takagi, H. W. Zandbergen, J. J. Krajewski, W. F. Peck, T. Siegrist, B. Batlogg, R. B. van Dover, R. J. Felder, K. Mizuhashi, O. J. Lee, H. Eisaki, and S. Uchida, *Nature (London)* **367**, 252 (1994).
- [24] K.-H. Müller, M. Schneider, G. Fuchs, and S.-L. Drechsler, in *Handbook of the Physics and Chemistry of Rare Earth*, edited by K. A. Gschneidner, J. G. Bünzli, and V. K. Pecharsky (North-Holland, Amsterdam, The Netherlands, 2008), Vol. 38, p. 175.
- [25] C. Mazumdar and R. Nagarajan, *Physica C* **514**, 173 (2015).
- [26] S. V. Shulga, S.-L. Drechsler, G. Fuchs, K.-H. Müller, K. Winzer, M. Heinecke, and K. Krug, *Phys. Rev. Lett.* **80**, 1730 (1998).
- [27] S. Mukhopadhyay, G. Sheet, P. Raychaudhuri, and H. Takeya, *Phys. Rev. B* **72**, 014545 (2005).
- [28] T. Yokoya, T. Baba, S. Tsuda, T. Kiss, A. Chainani, S. Shin, T. Watanabe, M. Nohara, T. Hanaguri, H. Takagi, Y. Takano, H. Kito, J. Itoh, H. Harima, and T. Oguchi, *J. Phys. Chem. Solids* **67**, 277 (2006).
- [29] B. Bergk, V. Petzold, H. Rosner, S.-L. Drechsler, M. Bartkowiak, O. Ignatchik, A. D. Bianchi, I. Sheikin, P. C. Canfield, and J. Wosnitza, *Phys. Rev. Lett.* **100**, 257004 (2008).
- [30] S. Manalo and E. Schachinger, *J. Low Temp. Phys.* **123**, 149 (2001).
- [31] M. Kawamura, R. Akashi, and S. Tsuneyuki, [arXiv:1610.07329v1](https://arxiv.org/abs/1610.07329v1).
- [32] T. Baba, T. Yokoya, S. Tsuda, T. Watanabe, M. Nohara, H. Takagi, T. Oguchi, and S. Shin, *Phys. Rev. B* **81**, 180509(R) (2010).
- [33] G. Behr, W. Löser, G. Graw, H. Bitterlich, J. Freudenberger, J. Fink, and L. Schultz, *J. Cryst. Growth* **198-199**, 642 (1999).
- [34] G. Behr, W. Löser, G. Graw, H. Bitterlich, J. Fink, and L. Schultz, *Cryst. Res. Technol.* **35**, 461 (2000).
- [35] B. Lüthi, *Physical Acoustics in the Solid State* (Springer, Berlin, 2005).
- [36] The upper critical field of 8.25 T was accurately determined from the torque (Fig. 2) and from specific-heat data (not shown).
- [37] L. H. Nguyen, G. Goll, E. Steep, A. G. M. Jansen, P. Wyder, O. Jepsen, M. Heinecke, and K. Winzer, *J. Low Temp. Phys.* **105**, 1653 (1996).
- [38] The additional nonsinusoidal feature appearing in the oscillating sound-velocity signal above about 12 T is caused by a rather strong higher-harmonic contribution in the  $\alpha$ -orbit oscillations (see also Fig. 1 in [13]).
- [39] K. Yamauchi, H. Katayama-Yoshida, A. Yanase, and H. Harima, *Physica C* **412-414**, 225 (2004).
- [40] The rather evolved hysteretic torque signal in the mixed state is a consequence of the torque-measurement technique. Indeed, the torque is given by  $\vec{\tau} = \vec{M} \times \vec{B}$ , which means that only the magnetization ( $\vec{M}$ ) component perpendicular to  $\vec{B}$  is detected. Since even the parallel component of  $\vec{M}$  depends strongly on many details (pinning centers, sweep rate, sample shape), the perpendicular component appears to be unpredictable and leads to the shown complicated field dependence.
- [41] M. Willemin, C. Rossel, J. Hofer, H. Keller, A. Erb, and E. Walker, *Phys. Rev. B* **58**, R5940 (1998); M. Willemin, A. Schilling, H. Keller, C. Rossel, J. Hofer, U. Welp, W. K. Kwok, R. J. Olsson, and G. W. Crabtree, *Phys. Rev. Lett.* **81**, 4236 (1998).
- [42] E. H. Brandt and G. P. Mikitik, *Phys. Rev. Lett.* **89**, 027002 (2002).
- [43] X. S. Ling, S. R. Park, B. A. McClain, S. M. Choi, D. C. Dender, and J. W. Lynn, *Phys. Rev. Lett.* **86**, 712 (2001).
- [44] M. Marziali Bermúdez, M. R. Eskildsen, M. Bartkowiak, G. Nagy, V. Bekeris, and G. Pasquini, *Phys. Rev. Lett.* **115**, 067001 (2015).
- [45] D. Shoenberg, *Magnetic Oscillations in Metals* (Cambridge University, Cambridge, England, 1984).
- [46] Here and in the following we only consider the contribution to the fundamental frequency.
- [47] Strictly speaking,  $m_c$  extracted from the temperature-dependent damping is renormalized by many-body interactions, whereas the mass in Eq. (1) is not (see [2]). This point is usually neglected as we do as well here.
- [48] The only difference in the field dependence between the amplitudes of the torque and magnetoacoustic quantum oscillations is an additional factor  $B$  for the torque data. See [45] and J. D. Wilde and D. G. de Groot, *J. Phys. F* **8**, 1131 (1978).
- [49] Any deviation from an ideal hexagonal flux-line lattice would lead to a stronger damping of the oscillating signal in the mixed state, as seen in the torque data.
- [50] J. I. Lee, T. S. Zhao, I. G. Kim, B. I. Min, and S. J. Youn, *Phys. Rev. B* **50**, 4030 (1994).
- [51] N. M. Hong, H. Michor, M. Vybornov, T. Holubar, P. Hundegger, W. Perthold, G. Hilscher, and P. Rogl, *Physica C* **227**, 85 (1994).
- [52] Even when unphysically neglecting  $R_{FL}$ , i.e., assuming a much larger  $\kappa$ , and using a lower bound for  $T_D$ ,  $\Delta_0$  would always be less than 1 meV using Eq. (3).
- [53] N. R. Werthamer, G. Helfand, and P. C. Hohenberg, *Phys. Rev.* **147**, 295 (1966); see Fig. 1 therein.
- [54] G. Fuchs, S.-L. Drechsler, N. Kozlova, M. Bartkowiak, J. E. Hamann-Borrero, G. Behr, K. Nenkov, H.-H. Klauss, H. Maeter, A. Amato, H. Luetkens, A. Kwadrin, R. Khasanov, J. Freudenberger, A. Köhler, M. Knupfer, E. Arushanov, H. Rosner, B. Büchner, and L. Schultz, *New J. Phys.* **11**, 075007 (2009).
- [55] Note that this plot is valid only above  $B_{c2}$  estimated using Eq. (4) when the residual superconductivity (here in the  $\alpha$  pocket) is induced by interband coupling.
- [56] S. V. Shulga and S.-L. Drechsler, *J. Low Temp. Phys.* **129**, 93 (2002).
- [57] K. Winzer and K. Krug, in *Rare Earth Transition Metal Borocarbides (Nitrides)*, edited by K.-H. Müller and V. Narozhnyi, Nato Science Series 2 Vol. 14 (Springer, New York, 2001), p. 63.
- [58] Thereby, Coulomb pseudopotentials  $\mu^*$  between 0.1 and 0.4 were determined using the Allan-Dynes  $T_c$  formula: P. B. Allen and R. C. Dynes, *Phys. Rev. B* **12**, 905 (1975).

- [59] C. L. Huang, J. Y. Lin, C. P. Sun, T. K. Lee, J. D. Kim, E. M. Choi, S. I. Lee, and H. D. Yang, *Phys. Rev. B* **73**, 012502 (2006).
- [60] K. Maki, P. Thalmeier, and H. Won, *Phys. Rev. B* **65**, 140502(R) (2002).
- [61] K. Izawa, K. Kamata, Y. Nakajima, Y. Matsuda, T. Watanabe, M. Nohara, H. Takagi, P. Thalmeier, and K. Maki, *Phys. Rev. Lett.* **89**, 137006 (2002).
- [62] T. Saito, K. Koyama, K. Magishi, and K. Endo, *J. Magn. Magn. Mater.* **310**, 681 (2007).